JOURNAL OF ELECTROMAGNETIC ENGINEERING AND SCIENCE, VOL. 23, NO. 5, 449~451, SEP. 2023

https://doi.org/10.26866/jees.2023.5.l.16
ISSN 2671-7263 (Online) · ISSN 2671-7255 (Print)

Efficient Clutter Cancellation Algorithm Based on a Suppressed Clutter Map for FMCW Radar Systems

Bong-seok Kim · Youngseok Jin · Jieun Bae · Eugin Hyun*

Abstract

This paper proposes an efficient clutter cancellation algorithm based on suppressed clutter map for frequency-modulated continuous wave radar systems. In conventional clutter cancellation algorithms based on clutter maps, range-Doppler maps are employed. However, if the radar cross section (RCS) of the targets is significantly lower than the RCS of the clutter, a problem may occur in that the targets may also be removed in the clutter-removal process. To solve this problem, the proposed algorithm creates a range-Doppler map to which the moving target indicator (MTI) algorithm is applied instead of the general range-Doppler map that does not include the MTI algorithm. The range-Doppler map, used after applying the clutter suppression filter, significantly reduces the clutter removal effect on targets in which RCS is relatively weak by suppressing the effect of relatively dominant clutter signals. The experimental results showed that the proposed algorithm detects weak targets that remain undetected by the existing map-based clutter-removal algorithm.

Key Words: Clutter Suppression, MTI, Radar, RCS, RD Map.

I. Introduction

In radar systems, clutter cancellation is one of the most challenging issues; thus, research in this realm, including clutter suppression filters, moving target indicator algorithms [1–4], and clutter cancellation algorithms using clutter maps [5], is in progress.

Meanwhile, in [2, 3], the researchers employed differences between chirps; thus, clutter was effectively cancelled. In [5], to suppress the effect of clutter, researchers used clutter maps based on range-Doppler (RD) maps. They first generated RD maps, or so-called clutter maps, several times in advance. By subtracting the generated clutter maps from the received signals, clutter is removed and the target parameters are estimated. However, in cases in which the radar cross section (RCS) of the target is significantly lower than that of the clutter, a problem may occur; the clutter-removal process may remove targets as well as clutter.

In this paper, to overcome this problem, the proposed algorithm creates an RD map after applying the clutter suppression filter instead of a general RD map. After the clutter suppression filter is applied, the RD map significantly reduces the clutter removal effect on targets, where RCS is relatively weak by suppression of the effect of relatively dominant clutter signals. To confirm the effectiveness of the proposed algorithm, experiments using 24-GHz radar systems were performed. The experimental results showed that the proposed algorithm could detect weak targets that remained undetected by the existing map-based clutter-removal algorithm.

II. System Model

This section considers the system model of a frequency-modulated continuous wave (FMCW) radar system. In this

Manuscript received December 19, 2022 ; Revised January 19, 2023 ; Accepted February 15, 2023. (ID No. 20221219-180J)
Department of Future Automotive Technology, Daegu Gyeongbuk Institute of Science and Technology
*Corresponding Author: Eugin Hyun (e-mail: braham@dgist.ac.kr)

model, L chirp signals were sequentially transmitted for N frames and received by K RX antennae. The beat signal was obtained by mixing the TX signal with the RX signal. At the k-th RX antenna, the l-th analog-to-digital convert (ADC) beat signal is denoted by $y_l^{(k)}[n]$ and is expressed as follows.

$$y_l^{(k)}[n] = \sum_{i=0}^{N-1} y_l^{(k,i)}[n]\, \Pi[n - LTi], \tag{1}$$

where $\Pi[n]$ is unit amplitude pulse and $y_l^{(k,i)}[n]$ is the beat signal at the i-th frame and expressed as follows:

$$y_l^{(k,i)}[n] = \sum_{m=1}^{M} a_m^{(i)} \exp\left(j2\pi \left(\underbrace{f_{D,m}^{(i)} lT}_{\text{Doppler}} - \underbrace{f_{b,m}^{(i)} nt_s}_{\text{Range}} + \underbrace{k\frac{\sin\theta_m^{(i)}}{2}}_{\text{Angle}} \right) \right) + w_l^{(k,i)}[n], \tag{2}$$

where $a_m^{(i)}$ is the complex amplitude of the m-th target at the i-th frame; T is the chirp duration; $f_{D,m}^{(i)}$ is the Doppler frequency due to the velocity of the m-th target; $f_{b,m}^{(i)}$ is the beat signal, that is, $f_{b,m}^{(i)} = \mu\tau_m^{(i)}$, where μ is the slope and $\tau_m^{(i)}$ is delay due to the distance of the m-th target; t_s is the sampling interval; $\theta_m^{(i)}$ is the angle of the m-th target; and $w_l^{(k,i)}[n]$ is the additive white Gaussian noise.

III. Conventional and Proposed Clutter Cancellation Algorithms Based on RD Map

This section addresses conventional and proposed clutter cancellation algorithms based on the RD map. Fig. 1 shows the structures of conventional and proposed algorithms, where the part boxed with solid lines is the conventional algorithm, and that boxed with dotted lines is the proposed algorithm. Both algorithms usually consist of a clutter-map-generation step and a detection step after clutter removal. In the first step, to generate the RD clutter map in the case of no target, 2D fast Fourier transform (FFT) was performed on $y_l^{(k,i)}[n]$ to sample and chirp domain indices, that is, n and l, and the generated RD maps were accumulated several times. In the second step, the clutter components acquired in the first step were removed to improve the target detection performance.

However, when the RCS of the target is significantly lower than that of the clutter, both the target and clutter components might be removed during the clutter-removal process. Therefore, in the proposed algorithm (Fig. 1), a clutter suppression filter was added between range profiling and Doppler profiling. This process had the effect of relatively increasing the RCS of the target, which was significantly lower than that of the clutter.

IV. Experimental Results

In this section, the performance improvement of the proposed algorithm was verified through experiments using 24-GHz

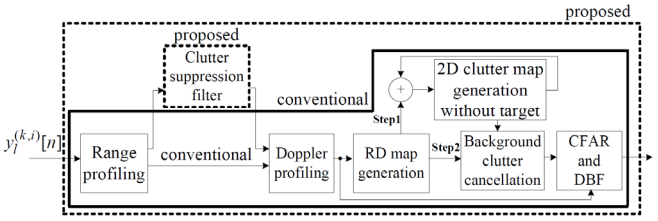

Fig. 1. Structure of conventional (solid line) and proposed (dashed line) algorithms. CFAR=constant false alarm rate, DBF=digital beamforming.

FMCW radar systems with 1 TX and RX antennae. Fig. 2 shows the configuration of the experiments, consisting of a 24-GHz FMCW radar front-end module with antennae and transceiver, a real-time signal logging module, and an algorithm based on MATLAB of PC. Two modules have been developed by the Radio Research Center for Advanced Intelligent Radar Sensor Technology (RRCAiRST) in Korea. The parameters for the experiments were as follows: bandwidth $B = 250$ MHz, chirp duration $T = 100$ μs, pulse repetition interval $T_{\text{PRI}} = 1$ μs, number of frames $N = 1{,}000$, TX power $P_{\text{TX}} = 10$ μW, and field-of-view of antenna = 90°.

Fig. 3 shows the environment for the experiment, that is, the scenario and photograph of the experimental equipment. Two walls were there on the sides and two doors at the front that were cluttered, and their RCSs were significantly higher compared to that of the target person. The target started from the space on the left, exited through the door, and returned to the radar.

Fig. 4 shows the results of range measurement according to the frame index. The figure shows following four cases: cases using and not using the clutter suppression filter (CSF) and cases using and not using the clutter map. In Fig. 4(a), neither

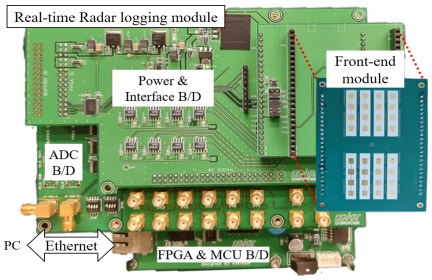

Fig. 2. Configuration of a 24-GHz FMCW radar experiment. FPGA =field-programmable gate array, MCU=microprogrammed control unit.

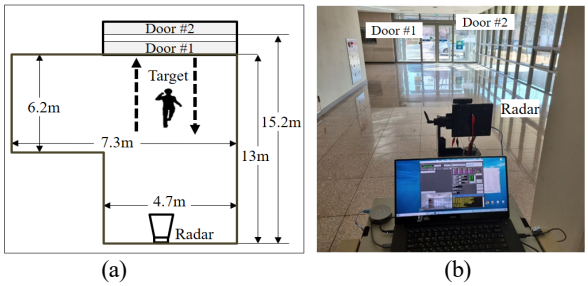

(a) (b)

Fig. 3. Environment for the experiment: (a) scenario and (b) photograph.

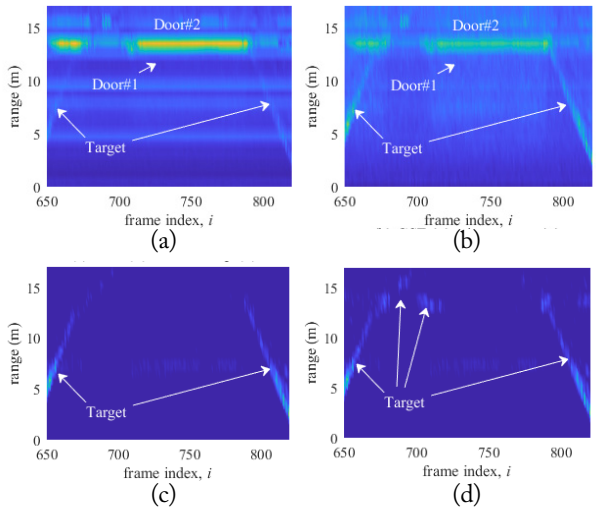

Fig. 4. Measurement results of range according to frame index: (a) CSF (×), clutter map (×); (b) CSF (o), clutter map (×); (c) CSF (×), clutter map (o); and (d) CSF (o), clutter map (o).

the CSF nor the clutter map was used. Because clutter was not removed, the doors with high RCS were dominant compared to the target, and the target was relatively insignificant. In Fig. 4(b), CSF was used but a clutter map was not used. Due to the effect of CSF, the intensity of the dominant doors in Fig. 4(a) became relatively small, and the intensity of the target, which was insignificant, became relatively large. However, it was difficult to detect the target around the door due to the door's residual effects. In Fig. 4(c), CSF was not used but a clutter map was used (i.e., the case of the conventional algorithm). Due to the effects of the clutter map, almost entire clutter was removed, and the target results were clearly visible. However, it can be seen that clutter corresponding to large RCS doors was removed, and the target was also removed. Hence, the target was not detected around the doors. The target is detected up to about 13 m and remains undetected when the range exceeds 13 m. Fig. 4(d) shows the results of using both the CSF and clutter map, that is, the proposed algorithm. Since the effects of the dominant clutter were suppressed by CSF, the target was detected around the door after clutter removal using a clutter map. In other words, the target is detected when the proposed algorithm is applied, even in the range of over 13 m, which was not detected in Fig. 4(c).

Fig. 5 shows a comparison between the conventional and proposed algorithms at $i = 680$ of RD maps obtained for doors

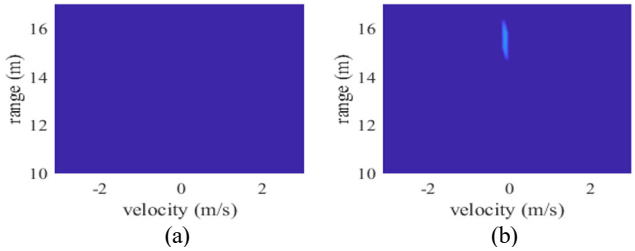

Fig. 5. Comparison of measured RD maps using (a) conventional (before) and (b) proposed (after) algorithms at frame index $I = 680$.

with high RCS. In Fig. 5(a), not only clutter was removed but also the target, so the target remained undetected in the conventional algorithm, as expected from Fig. 4. In contrast, the proposed algorithm clearly detects the target around the doors in Fig. 5(b).

V. Conclusion

We proposed an efficient clutter cancellation algorithm based on a suppressed clutter map and CSF. The proposed algorithm significantly reduced the dominant clutter effect by applying a CSF between range profiling and Doppler profiling. As a result, the problem of targets remaining undetected around large RCS clutter was solved.

This work was supported in part by the Institute for Information and Communications Technology Planning and Evaluation (IITP) grant funded by the Korea government (MSIT) (No. 2019-0-00138, Development of Intelligent Radar Platform Technology for Smart Environments).

References

[1] P. Huang, H. Yang, X. G. Xia, Z. Zou, X. Liu, and G. Liao, "A novel sea clutter rejection algorithm for spaceborne multichannel radar systems," *IEEE Transactions on Geoscience and Remote Sensing*, vol. 60, article no. 5117422, 2022. https://doi.org/10.1109/TGRS.2022.3204324

[2] B. S. Kim, Y. Jin, S. Kim, and J. Lee, "A low-complexity FMCW surveillance radar algorithm using two random beat signals," *Sensors*, vol. 19, no. 3, article no. 608, 2019. https://doi.org/10.3390/s19030608

[3] E. Hyun, Y. S. Jin, and J. H. Lee, "A pedestrian detection scheme using a coherent phase difference method based on 2D range-Doppler FMCW radar," *Sensors*, vol. 16, no. 1, article no. 124, 2016. https://doi.org/10.3390/s16010124

[4] C. Gouveia, J. Vieira, and P. Pinho, "Motion detection method for clutter rejection in the bio-radar signal processing," *International Journal of Electronics and Communication Engineering*, vol. 12, no. 8, pp. 518-526, 2018. https://doi.org/10.5281/zenodo.1340482

[5] B. Xu, Y. Chen, H. Gu, and W. Su, "Research on a novel clutter map constant false alarm rate detector based on power transform," *Radioengineering*, vol. 31, no. 1, pp. 114-126, 2022. https://doi.org/10.13164/re.2022.0114